Physical Sciences and Technology. Vol. 9 (No. 1-2), 2022: 13-20

IRSTI 27.35.51 https://doi.org/10.26577/phst.2022.v9.i1.02

Effect of laminar and turbulent flow on the collective motion of plasma microdischarges at atmospheric pressure

A.I. Ashirbek[1*], E.A. Usenov[1,2], M.K. Dosbolaev[3], M.T. Gabdullin[4] and T.S. Ramazanov[3]

[1]Institute of Applied Science and Information Technologies, Almaty, Kazakhstan
[2]NNLOT, Faculty of Physics and Technology, Al-Farabi Kazakh National University, Almaty, Kazakhstan
[3]IETP, Faculty of Physics and Technology, Al-Farabi Kazakh National University, Almaty, Kazakhstan
[4]Kazakhstan-British Technical University, Almaty, Kazakhstan
*e-mail: azamat.ashirbeck@gmail.com

(Received 25 January 2022; received in revised form 12 March; accepted 5 April 2022)

Dielectric barrier discharge (DBD) is used for many important applications in various sectors of science and technology. For example, for ozone generation, surface modification of polymers, in plasma medicine, and for decomposition of heavy volatile organic compounds. Nowadays, one of the actual problems is getting of uniformity of discharge distribution for high quality treatment of materials surfaces. To achieve uniform distribution of the discharge, several methods are available, one is to use different types of noble gases, and another is to use AC power supply with frequency varied in wide range. But besides this, another of the potential methods for obtaining a uniformly distributed discharge is to blow through the discharge gap flow of air. This method was used in this paper to conduct experiments which consisted of oscilloscoping voltage and current values, high-speed imaging, also gas flow simulation for comparison with the experiments. The obtained results show the dynamics of microdischarge motion in laminar and turbulent flow regimes, which supported by flow simulation.

Key words: plasma, dielectric barrier discharge, gas flow, gas flow modelling, microdischarges.
PACS numbers: 34.80.Bm, 34.80.Dp, 51.50.+v, 52.80.Dy.

1 Introduction

Dielectric barrier discharge (DBD), also called ‘’barrier’’ or ‘’silent’’ discharge, is a typical nonequilibrium AC discharge at atmospheric pressure [1]. The most important characteristic of the dielectric barrier discharge is that conditions for the generation of nonequilibrium plasma can be provided much more easily [2] compared to other types of alternative discharges [3] such as low-pressure discharges, high-pressure pulsed discharges or atmospheric pressure uniform arcs. Its simplicity in terms of geometric configuration, operating medium and operating parameters is irreplaceable. The conditions optimized in laboratory experiments can easily be adapted to large industrial equipments. The presence of a dielectric is the key to the limiting the current of the discharge. It limits the charge transported in the discharge, i.e. it limits the current flow into the system and almost uniformly distributes the discharge over the entire electrode area. Recently two main types of DBD designs have been proposed: volume barrier discharge (VBD), and surface barrier discharge (SBD)[4]. VBD consists of two parallel dielectric plates with electrodes mounted externally or two electrodes on one side of the dielectric. SBD device has a dielectric surface with a small but elongated electrode on one side of the dielectric and a metallic electrode coated on the opposite side [5,6]. Such devices are advantageous for industrial use because vacuum equipment can be avoided and DBD-based devices operate in the atmospheric pressure range.

In the electrode gap, following an electrical breakdown, current pulses or a charged plasma channel are generated. These current pulses are shaped like filaments, hence the term “filamentary discharge” could be used. These filament channels are also called microdischarges (MD), because the current through the filaments is very low. The location of the occurrence of microdischarges on the electrode surface is random. However, after ignition, the microdischarges remain at this point for a long time (periods) – up to 300 half-periods at an applied voltage of 100 kHz (more precisely, the microdischarges slowly move through the monitoring area). This means that the displacement of the microdischarge in one half-period is less than 0.25 μm, which is negligible, compared to the diameter of the microdischarge. Thus, it can be concluded that there is a spatial memory in the microdischarge in the stationary DBD, the microdischarge in each subsequent half-period does not jump to an arbitrary point on the electrode surface, but appears exactly at the point of the surface where it was in the previous half-period. Currently, there is no standard point of view regarding the temporal and spatial 'memory' of microdischarges. The cause of the spatial memory effect for a subsequent microdischarge is the residual surface charge deposited on the barrier by a previous microdischarge. This charge can locally increase the electric field during the next half-period and hence provide a gas breakdown (i.e. the occurrence of a subsequent MD), preserving the site of occurrence.

The influence of air (gas) flow on the dynamics of MD channels in DBD is of great interest both from the point of view of fundamental research and for solving applied problems. At present one of the urgent tasks is to obtain uniform discharge distribution in DBD for high quality treatment of material's surfaces. To obtain such a discharge distribution there are several approaches, one of them is to use various types of noble gases and the other is to use AC power supply with high frequency. But apart from this, another potential method to obtain a uniformly distributed discharge in DBD is by blowing out the discharge gap with an air flow [7-10]. DBD in a gas flow is actively used in so-called cold plasma jets (cold plasma jets) in the field of plasma medicine and surface treatment of various materials. The presence of gas flow in the discharge gap allows efficient cooling of the discharge walls and the plasma channel itself to room temperature and controlling plasma chemical processes to obtain the desired biologically active components. Another application of gas flow in DBD is active control of gas flow dynamics in plasma actuators in order to stabilize turbulence at the interface with the surface of solids. These studies are mainly carried out with the help of surface DBD in the air atmosphere and have great perspectives for aeronautical applications [11]. Microdischarge DBD with actively blown gas in the discharge gap is often used in reactors for plasma-chemical decomposition of heavy volatile organic compounds (VOC) [12], for carbon dioxide (CO2) utilization and synthesis gas generation [13], and for dry methane reforming and hydrogen production. From this it can be concluded that studies of the effect of gas flow on the dynamics of micro-discharge channels for different modes of flow itself is an relevant task. In the present work we have carried out experiments to determine the effect of gas flow velocity on the structural and dynamic characteristics of microdischarge channels. Laminar and turbulent modes of blown gas flow into the discharge interval of a DBD with flat-parallel geometry of electrodes were considered. The trajectories of microdischarge channels have been determined by means of video imaging. In case of laminar mode of gas flow, the microdischarge channels move strictly in the central region and follow the direction of gas flow. For the turbulent mode, the presence of vortices in the trajectories of microdischarge channels is revealed. The corresponding gas flows have been simulated with the Comsol Multiphysics software package for specific experimental conditions, and have been compared with real trajectories of MD channels. The results showed that the MD channels completely follow the direction of gas flow in the discharge gap for laminar mode. In the turbulent mode, vortices and backward to the flow collective motion of MD channels are also observed.

2 Experimental set-up

A gas-discharge cell with a flat-parallel configuration, as shown in Figure 1, has been constructed for experiments with DBD. The design of electrodes in discharge cells has a flat geometry and consists of two parallel quartz plates, which play the role of dielectric ($\varepsilon = 3.5$), with parameters of 60mm x 60mm and a height of 2 mm. The air gap between the surfaces of the plates is $h = 3$ mm. One plate has a transparent conductive glass top coated with indium tin oxide (ITO), and is earthed via a low-inductive current shunt with resistance $R = 51$ Ohm. An aluminum foil is applied to the back of the second quartz plate and a high voltage from a PVM 500 sinusoidal generator is fed through it. Given the dimensions of the dielectric inserts for fixing the wires, the area of the discharge zone is 40x40 mm^2. The frequency and amplitude of the sinusoidal voltage varies between 20-30 kHz and 10-15 kV respectively.

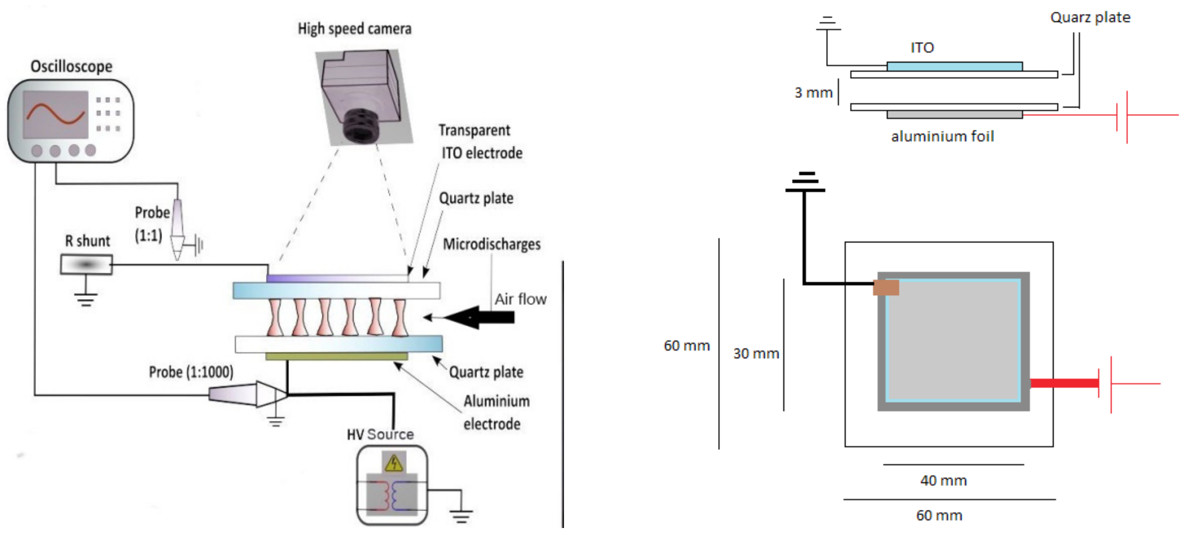

(a) (b)

Figure 1 – Scheme of the experimental setup (a) and geometry of the gas discharge cell (b).

All experiments were performed in a stream of air (at room temperature) directed along the walls of the plate. The gas flow velocity was varied up to 30 m/s inside the cell. Measurement of flow velocity was performed at the cell outlet, using Pitot tube with diameter 0.5 mm, equipped with micromanometer MMN-2400 (5)-1. The schematic in Figure 1 b explains the synchronized operation of a sinusoidal high voltage, a 4 channel digital oscilloscope (LeCroy WJ354A, 500 MHz) and a high-speed camera (Phantom VEO 710S). Microdischarge was photographed, with an overhead view through a transparent ITO conductor and a quartz plate. The whole circuit is started by switching on the key K1, which supplies the high voltage sine wave generator. The signal from the delay generator, received from the power supply, starts the high speed camera at the same moment. The discharge voltage was measured with a Tektronix P6015 high voltage divider (1:1000). The discharge current was measured with a current shunt.

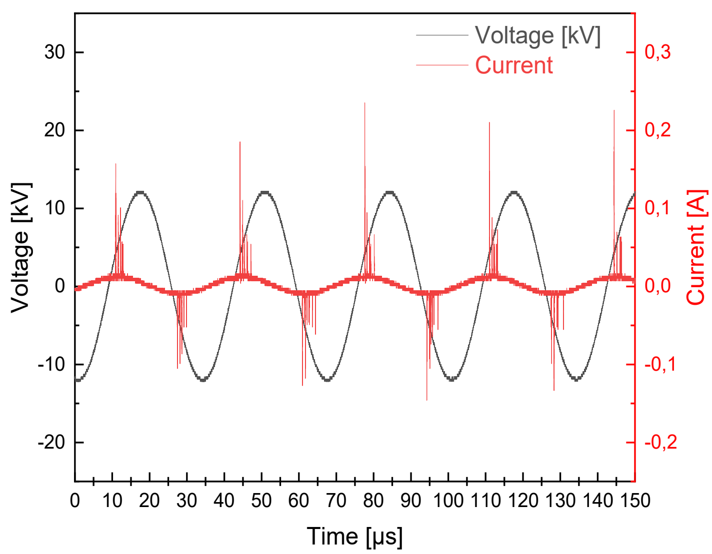

Figure 2 – Typical dynamic volt-ampere oscillogram of the DBD with plane-parallel electrode geometry. Each current spike in the oscillogram corresponds to the occurrence of one or more microdischarge channels.

Figure 2 shows a typical voltage and current waveform of a volumetric barrier discharge. From this graph, it can be seen that, the voltage and current were indicated black and red color respectively. The highest number of voltage was approximately 12.5 kV, and with frequency 28.6 kHz. The current consisted of two parts, which involve a sinusoidal part called conductivity current and sharp ends called bias current.

3 Results

The resulting images for DBD without airflow, at h = 3 mm for a flat-parallel electrode geometry are shown in Figure 3. The images were acquired using a high-speed camera with a frequency of 25000 frames per second and an exposure time of 40 µs. Also, the number of microdischarges is calculated from 500 pictures and averaged.

In Figure 3 (a) the voltage U applied to the electrodes is 9.7 kV and the breakdown voltage is 4.8 kV. The average number of microdischarges is equal to 17. Further in the Figure 3 (b) U is equal to 10,45 kV, in this section more or less stable number of microdischarges is formed equal to 31. Increasing the U to 11.61 kV, in figure 3 (c) we get a fully filled gas-discharge cell in which the number of microdischarges is 53. And when U reaches 12.57 kV in a fully filled gas discharge cell more microrischarge appear and so the distance between the microrischarge decreases, as indicated in the Figure 3 (d). It can also be seen that on a maximally filled cell, the arrangement of microdischarges have a strict pattern and is an example of a self-organized structure [14,15].

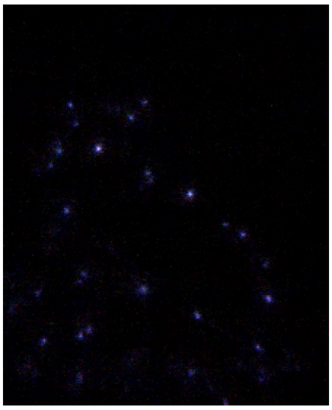

U=9.7 kV
(a)

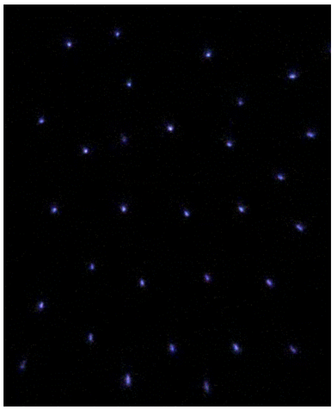

U=10.45 kV
(b)

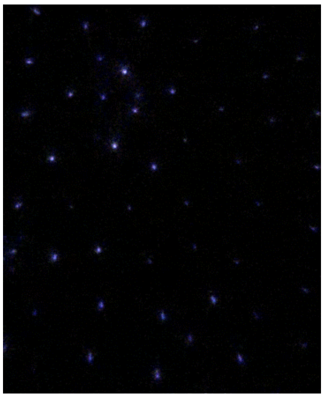

U=11.61 kV
(c)

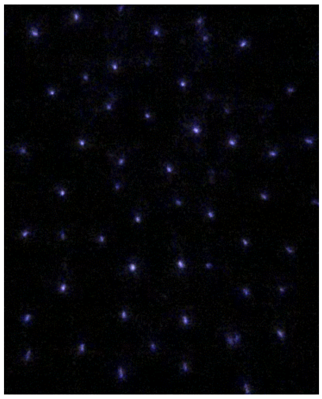

U=12.57 kV
(d)

Figure 3 – Photographs of the VBD (top view) obtained using high-speed video recording without airflow, with different applied voltages, at h = 3 mm. and exposure time of 40 µs.

4 Modelling results

When affected by the air flow [16-20], the microdischarges begin to move in the direction of the flow. By observing this phenomenon, it can be seen that depending on the flow velocity, the movement of the microdischarge has a different character. It is known that there are three types of gas dynamic flow regimes, changes between regimes are depended on the flow velocity of the gas. For this geometry, the Reynolds number for all three types of flow modes at certain flow velocities has been calculated. For clarity, microdischarge motions in laminar and turbulent flow are shown in Figure 4 below. In the figure 4 (a), it's first case, the flow velocity is 5 m/s and Reynolds number is 2100, which corresponds to laminar mode. In the figure 4 (b), it's second case, the flow velocity is 30 m/s and Reynolds number is 6200, corresponding to turbulent mode. Both figures were obtained at 24 fps, with an exposure time of 41 ms.

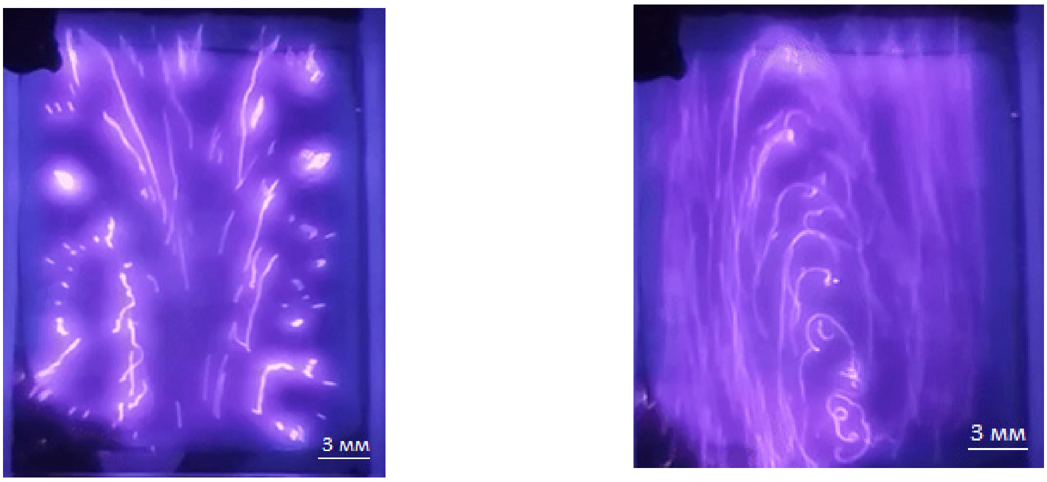

(a) (b)

Figure 4 – MD motion in laminar flow (a) and turbulent flow (b), frame rate 24 fps, exposure time 41 ms.

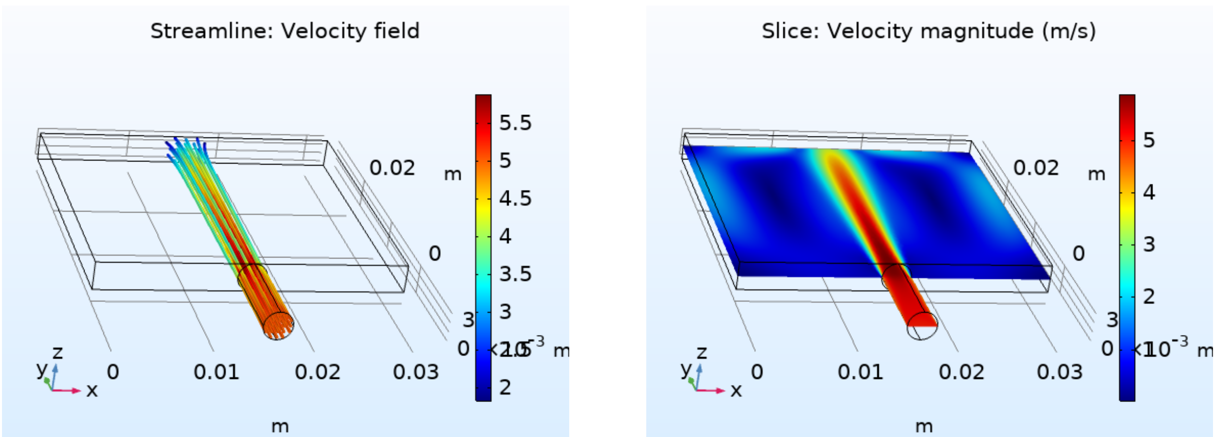

2(a) (b)

Figure 5 – Visualization of airflow in laminar mode, flow lines (a), surface velocity distribution (b).

Gas flow was modelled using the Comsol Multiphysics software. The Computational Fluid Dynamics (CFD) package was used for this purpose. The area between the active electrodes through which air is blown was chosen as the calculation area. The results are shown below as flow visualizations and as graphs.

Figure 5 (a) shows streamlines, i.e. flow lines, and Figure 5 (b) shows the velocity distribution of the gas flow in the interelectrode volume. The velocity values can be determined from the color scale on the right side of both figures. As the simulation results show, the maximum velocity value is 6 m/s. It can be seen from the flow visualization figure that at low velocities, the flow is uniform, but the area covered is limited. That is, the flow lines do not cover the entire inter-electrode area, but only that part which is coaxial to the inlet channel.

An increase in flow velocity leads to a transition from laminar to turbulent gas dynamic mode. Looking in detail at the flow simulation results in the turbulent mode, it can be seen that the flow lines gradually start to shift to the left side, then reaching the edge of the electrodes, passing along it, as shown in Figure 6(a). The velocity distribution itself over the electrode area is shown in Figure 6(b). The average flow velocity is in the range of 30-35 m/s. The flow velocity through the tube at the inlet of the discharge cell is 30 m/s. Further, with expansion of the discharge volume, the flow velocity reduces significantly and reaches 15-20 m/s at the exit through the inter-electrode space. It can also be noticed that near the opposite wall of the discharge cell the flow velocity starts to increase, indicating the occurrence of vortices inside the cell.

On the right edges of both figures are indicators that shows the velocity at a certain point on a color scale. When the gas velocity reaches turbulent values, the movement of the MD is vortex-like, as are the flow lines of the blown air.

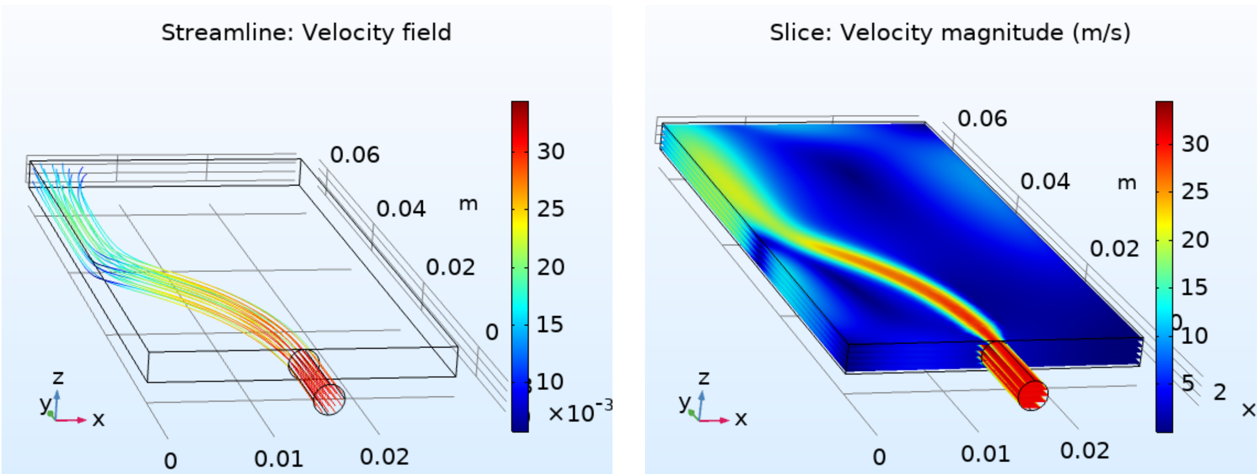

(a) (b)

Figure 6 – Visualization of airflow in turbulent mode.
Flow lines (a) and surface velocity distribution (b).

Figure 7 shows the velocity line cutting plots at different distances from the inlet channel, which are derived from figures 5 (a) and 6 (a). For laminar flow, (Figure 7a) three lines have selected and their positions from electrode width are 10 mm, 20 mm, 30 mm. The inlet channel is located at the position 17 mm of electrode length. As the electrode width position increased, the speed value of flow decreased, it can also be seen in the decrease in velocity peak along the inlet channel axis. At the same time closer to the walls the flow velocity starts decreasing and reaches some peak near the side walls of the discharge cell. At a position 30 mm from electrode width, the gas flow velocity increases along the edges of the main flow and there is a tendency for the flow to be more evenly distributed. For turbulent flow, Figure 7 (b), similar to the first case, 3 lines are chosen, but with different distances from the electrode widths of 15 mm, 30 mm and 50 mm. It can be seen that the velocity near the inlet channel is at its maximum and then the velocity peak shifts closer to the walls. This observation indicates the presence of eddies in the air flow lines and the formation of backward flow.

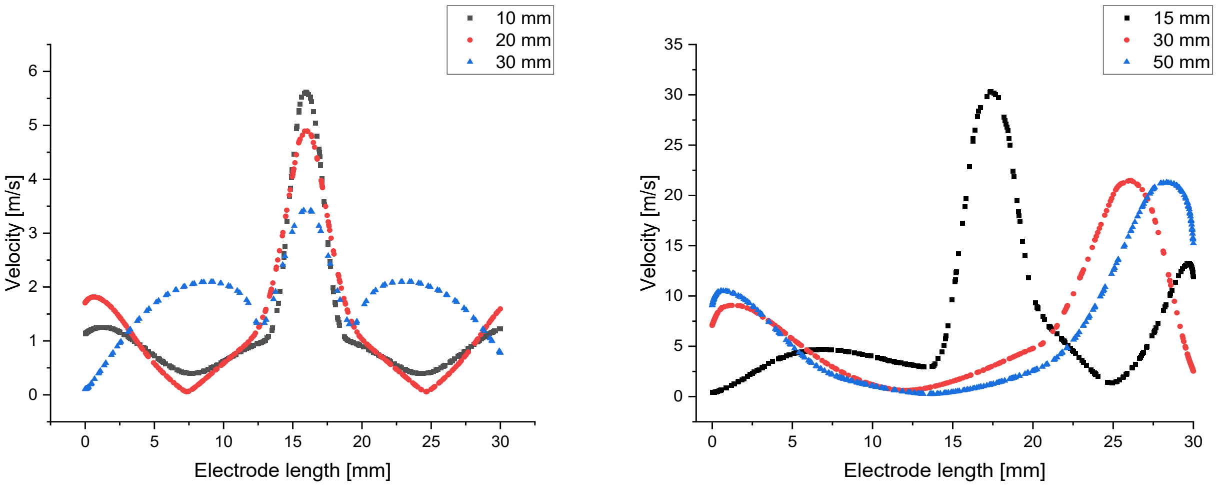

(a) (b)

Figure 7 – Velocity line slice graph at different distances from the inlet channel (a) for laminar flow, (b) for turbulent flow.

It is necessary to pay attention to the collective motion of MD's in the discharge gap and the similarity of their trajectory and gas flow lines at different gas-dynamic regimes. The simulation results obtained in laminar mode (Figure 5) completely repeat the trajectory of gas flow lines. The MD channels move only along the central axis of the inlet channel, with only some perturbations away from this axis. In the turbulent regime, the collective motion of MDs has a vortex-like character, which is consistent with the simulation results. In both cases, neutral atoms and molecules of the blown air in the flow transfer momentum to the active particles of the plasma channel (ions, excited atoms) through frequent collisions. In this case, the volume residual charges of the microdischarge channel begin to move along the flow and create a new location of the plasma on the electrode surface. Despite the discrete structure of the microdischarge channels, when imaging with relatively long exposure times, the trajectory and motion of the MD channels appears to be continuous. Our results further confirm the possibility of controlling the collective dynamics of the MD channels by airflow and the importance of gas-dynamic flow regimes for this purpose.

5 Conclusions

Careful analysis of the presented results on DBD microdischarge in gas flow shows that the overall discharge behavior, also the dynamics and structure of the MD completely change with increasing flow rate, as has been shown under different flow regimes. In this paper, results have been obtained on the MD dynamics in a flat surface multi-layer DBD and compared with the flow simulation results on Comsol. The discharges have special electrode arrangements in the form of "flat parallel plate" and are generated by a variable (27-32 kHz) sinusoidal voltage. Rapid visualization of the filaments and their synchronization with electrical diagnostics using an oscilloscope show that the discharge has different phases depending on the flow rate and gas-dynamic regimes. The obtained results of simulation of gas flow in the discharge gap are similar to the movement of MD under different gas-dynamic regimes. Comparison of experimental results with simulation results shows that the microdischarges move uniformly along the flow direction at laminar flow velocities. However, as the flow velocity increases up to turbulent mode, the MD motions have a vortex-like character. Directional air flow strongly influences the dynamics of microdischarge channels in the DBD and allows studying different properties of the discharges and the possibility of controlling the collective dynamics of MDs.

Acknowledgements

This work was supported by grant AP09258963 from the Science Committee of the Ministry of Education and Science of Kazakhstan

References

1. R. Brandenburg. Dielectric barrier discharges: Progress on plasma sources and on the understanding of regimes and single filaments // Plasma Sources Sci. Technol. Leibniz Institute for Plasma Science and Technology (INP Greifswald), Felix-Hausdorff-Strasse 2, Greifswald, D-17489, Germany: Institute of Physics Publishing. – 2017. – Vol. 26. – № 5. – P.053001.
2. E.A. Usenov et al. The memory effect of microdischarges in the barrier discharge in airflow // Plasma Phys. Reports. – 2020. – Vol. 46. – № 4. – P. 459–464.
3. O. V. Penkov et al. A review of recent applications of atmospheric pressure plasma jets for materials processing // J.Coatings Technol. Res. – 2015. – Vol. 12. – № 2. – P. 225–235.
4. Y.A. Ussenov et al. Dust particle synthesis by the combined plasma source at atmospheric pressure // IEEE Trans. Plasma Sci. Institute of Electrical and Electronics Engineers Inc. – 2019. – Vol. 47. – № 8. – P. 4159–4164.
5. Y. Ussenov et al. Particle formation during deposition of SiOx nanostructured thin films by atmospheric pressure plasma jet // Jpn. J. Appl. Phys. – 2020. –Vol. 59(3). – P. 14-23.
6. T. Jingfeng, W. Liqiu, H. Yuxin, S. Jian, Y. Daren, Z. Chaohai**.** Repetitive **n**anosecond **v**olume **di**scharges under airflows// Plasma Science and Technology. – 2016. – Vol. 18. – P. 273.
7. Fan Z., H Qi., Y. Liu, H. Yan, Ch. Ren**.** Investigation of airflow effects on the dielectric barrier discharge with single/double discharge channel arrangement// Physics of Plasmas. – - 2016. – Vol. 23. – P. 123520.
8. Z. Fan, H. Yan, Y. Wang, Y., H. Liu Guo, Ch. Ren**.** Effect of airflow on the space-time distribution of filaments in dielectric barrier discharge at atmospheric pressure// Physics of Plasmas. – 2018. – Vol. 25. – P. 053517.
9. K. H. Schoenbach, K. Becker**.** Pressure effect on a tandem hollow cathode discharge in argon// Eur. Phys. J. D. – 2016. – Vol. 70. – P. 29.
10. Yu. S. Akishev, M. Yu. Zaitsev, V. A. Kopiev, A. V. Petryakov, N. I. Trushkin. Influence of a barrier discharge on the gas-dynamic parameters of the plasma jet formed by it// Applied Physics. – 2018. – Vol. 6. – P. 14. (In Russian).
11. K. Fujii. Three flow features behind the flow control authority of DBD plasma actuator: Result of high-fidelity simulations and the related experiments// Applied Sciences. – 2018. – Vol. 8. – P. 546
12. S. P. Das, G. Dalei, A. A Barik. Dielectric barrier discharge (DBD) plasma reactor// IOP Conf. Series: Materials Science and Engineering. – 2018. – Vol. -P. 410.
13. A. Ozkan, T. Dufour, T. Silva**.** How do the barrier thickness and dielectric material influence the filamentary mode and CO_2 conversion in a flowing DBD?// Plasma Sources Science & Technology. – 2016. – Vol. 25. – No 2. – P. 11.
14. W. Fan, Z. Sheng, L. Dong, F. Liu, X. Zhong, Y. Cui, F. Hao, T. Du**.** Formation of side discharges in dielectric barrier discharge // Scientific Reports. – 2017. – Vol. 7. – No 8368.
15. **E. H. Matlis, T. C. Corke, B. Neiswander, A. J. Hoffman**. Electromagnetic wave transmittance control using self-organized plasma lattice metamaterial// Journal of Applied Physics. – 2018. – Vol 124. – P. 093104.
16. J. F. Tang, M. Tang, D. S. Zhou, P. T. Kang, X. M. Zhu, C. H. Zhang**.** Effect of airflow on the space-time distribution of filaments in dielectric barrier discharge at atmospheric pressure // Plasma Sci. Technol. – 2019. – Vol 21. -P. 044001.
17. P. Peschke, S. Goekce, P. Leyland, P. Ott**.** Investigation of nanosecond pulse dielectric barrier discharges in still air and in transonic flow by optical methods // J. Phys. D – 2016. – Vol. 49. – 025204.
18. Yu. Akishev, O. Goossens, T. Callebaut, C. Leys**,** A. Napartovich, N. Trushkin**.** The influence of electrode geometry and gas flow on corona-to-glow and glow-to-spark threshold currents in air // J. Phys. D – 2001. – Vol. 34 – P. 8.
19. Y. S. Akishev, G. Aponin, A. Balakirev, M. Grushin, V. Karalnik, A. Petryakov, N. Trushkin**.** Role of the volume and surface breakdown in a formation of microdischarges in a steady-state DBD // Eur. Phys. J. D – 2011 Vol. 61. – P. 421.
20. R. Tschiersch, S. Nemschokmichal, M. Bogaczyk, J. Meichsner**.** Self-stabilized discharge filament in plane-parallel barrier discharge configuration: formation, breakdown mechanism, and memory effects // J. Phys. D – 2017 – Vol. 50 – 415206.